Dyes and Pigments 82 (2009) 258–267

Contents lists available at ScienceDirect

Dyes and Pigments

journal homepage: www.elsevier.com/locate/dyepig

The relationship between solid-state fluorescence intensity and molecular packing of coumarin dyes

So-Yeon Park [a], Masahiro Ebihara [b], Yasuhiro Kubota [a], Kazumasa Funabiki [a], Masaki Matsui [a,*]

[a] Department of Materials Science and Technology, Faculty of Engineering, Gifu University, Yanagido, Gifu 501-1193, Japan
[b] Department of Chemistry, Faculty of Engineering, Gifu University, Yanagido, Gifu 501-1193, Japan

ARTICLE INFO

Article history:
Received 14 November 2008
Received in revised form
17 January 2009
Accepted 19 January 2009
Available online 3 February 2009

Keywords:
Coumarin
Solid-state fluorescence
X-ray crystallography

ABSTRACT

The solid-state fluorescence intensity of coumarin dyes depends on the substituents present at the 4- and 7-positions. 7-(Diethylamino)coumarins showed higher solid-state fluorescence quantum yield ($\Phi_f(ss) = 0.29–0.40$) than 7-aminocoumarins (0.01). In the case of julolydyl coumarins, a 4-methyltetramethyljulolydyl derivative also displayed high $\Phi_f(ss)$ (0.34), this being greater than that observed for both 4-(perfluoroalkyl)tetramethyljulolydyl (0.09 and 0.10) and 4-methyljulolydyl derivatives (0.01). X-ray crystallographic analysis suggested that coumarin dyes bearing network hydrogen bonds and/or π–π stacking show weak solid-state fluorescence whereas coumarin dyes having isolated monomer- and dimer-type stacking show intense fluorescence. 4-(Perfluoroalkyl)tetramethyljulolydyl derivatives displayed medium fluorescence intensity owing to isolated monomer-type packing with little intermolecular interactions operating between adjacent molecules.

1. Introduction

It is of significance to study the solid-state fluorescence of organic compounds from the view point of their applications to emitters in organic electroluminescence devices (OLED) and solid-state dye laser. Though number of organic compounds show fluorescence in solution, strongly solid-state fluorescent compounds are limited. Recently, new compounds such as dicyanopyrazines [1], 5-aryl-2,2′-bipyridyls [2], diazepines [3], heterocyclic quinol-type fluorophores [4–7], 2-aryl-3-hydroxyquinolones [8], fumaronitriles [9,10], dithieno [3,2-*b*:2′,3′-*d*]pyrroles [11], oxadiazoles [12], diborylphenylenes [13], pyrones [14], and perylenediimides [15] have been reported to show solid-state fluorescence. However, in the case of practically used fluorophores, no systematic studies on solid-state fluorescence have been reported so far. Coumarins are well-known fluorescent compounds used as sensors [16], fluorescence labeling reagents [17,18], emitters in solid dye laser [19,20] and OLED. Hindered coumarin dyes such as 7-di(2-substituted arylamino)-4-methylcoumarins act as good emitters in OLED due to intense fluorescence in solid state [21–23]. 7-(Dialkylamino)coumarins are typical and important compounds to show intense fluorescence. Though coumarin dyes having a julolydyl moiety are also important compounds as strong fluorophores in solution, little is known for their solid-state fluorescence. 4-(Perfluoroalkyl)coumarin dyes are also interesting compounds as the bathochromic derivatives. In this report, we systematically examined the relationship between solid-state fluorescence intensity and molecular packing of typical coumarin dyes.

2. Results and discussion

2.1. Materials

Scheme 1 shows coumarin dyes used in this study. Coumarin dyes **1** and **3** were commercially available compounds obtained from market. Coumarin dyes **2**, **4**, **6**, **7**, and **8** were synthesized as described in literature [24]. As the measured melting points of **6** and **7** were not same as reported ones, their TG-DTA, MS, ^{1}H NMR, and elemental analysis were performed. The MS, ^{1}H NMR, and elemental analysis data supported the structures. Coumarin dyes **5** and **9** are new compounds. They were synthesized by the reaction of substituted phenols with ethyl (pentafluoropropanoyl)acetate in the presence of zinc chloride as shown in Schemes 2 and 3.

2.2. UV–vis absorption and fluorescence spectra of coumarin dyes in solution

The UV–vis absorption and fluorescence spectra of **1**–**9** in dichloromethane are shown in Fig. 1. The results are also summarized in Table 1. The UV–vis absorption maxima (λ_{max}) of

* Corresponding author. Tel.: +81 (0)58 293 2601; fax: +81 (0)58 293 2794.
E-mail address: matsui@apchem.gifu-u.ac.jp (M. Matsui).

0143-7208/$ – see front matter © 2009 Elsevier Ltd. All rights reserved.
doi:10.1016/j.dyepig.2009.01.014

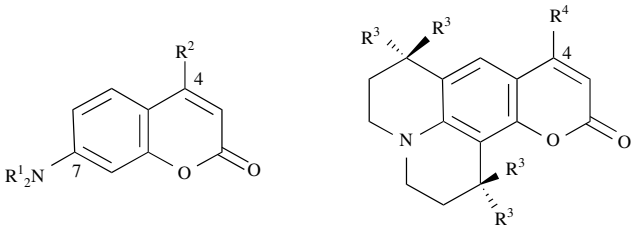

1: $R^1 = H$, $R^2 = Me$
2: $R^1 = Et$, $R^2 = Me$
3: $R^1 = H$, $R^2 = CF_3$
4: $R^1 = Et$, $R^2 = CF_3$
5: $R^1 = Et$, $R^2 = C_2F_5$

6: $R^3 = H$, $R^4 = Me$
7: $R^3 = Me$, $R^4 = Me$
8: $R^3 = Me$, $R^4 = CF_3$
9: $R^3 = Me$, $R^4 = C_2F_5$

Scheme 1. Materials.

4-(perfluoroalkyl)coumarin dyes **3** (360 nm), **4** (401), **5** (409), **8** (417), and **9** (426) were more bathochromic than the 4-methyl derivatives **1** (336), **2** (372), **6** (385), and **7** (382). The λ_{max} of 7-(diethylamino) and julolydyl derivatives **2** (372), **4** (401), **5** (409), **6** (385), **7** (382), **8** (417), and **9** (426) were more bathochromic than the 7-aminocoumarin dyes **1** (336) and **3** (360). These results come from intramolecular charge-transfer chromophoric system of the coumarins from (dialkylamino)aryl to lactone moieties [25]. The molar absorption coefficients (ε) of 7-substituted derivatives **2**, **4**, **5**, **6**, **7**, **8**, and **9** were larger than those of 7-amino derivatives **1** and **3**. The fluorescence maximum (F_{max}) was more bathochromic in the order of coumarins: **8** (510), **9** (517) > **5** (480), **4** (478) > **3** (439), **6** (440), **7** (441) > **2** (424) > **1** (397). Thus, both the introduction of electron-withdrawing perfluoroalkyl group at the 4-position and rigid julolydyl moiety at the 7-position were effective to show bathochromic F_{max}. The Stokes shifts of 4-perfluoroalkyl derivatives **3** (79 nm), **4** (77), **5** (71) **8** (93), and **9** (91) were slightly larger than those of 4-methyl derivatives **1** (61), **2** (52), **6** (56), and **7** (59). The Φ_f(sol), which represents the fluorescence quantum yield in solution, of **1**–**9** was very high (0.77–0.95).

2.3. Solid-state fluorescence of coumarin dyes

The solid-state fluorescence spectra of **1**–**9** are shown in Fig. 2. The results are also listed in Table 1. The spectra were more bathochromic compared with those in dichloromethane. For example, the F_{max} of **5** in solid state was observed at 512 nm, whereas that in dichloromethane at 480 nm, suggesting intermolecular interactions in solid state. The F_{max} of 4-perfluoroalkyl derivatives **3** (476 nm), **4** (522), and **5** (512) was more bathochromic than those of 4-methyl derivatives **1** (450) and **2** (432). The Φ_f(ss)/Φ_f(sol) ratio, where Φ_f(ss) represents the quantum in the solid state, was used to compare the fluorescence intensity. The Φ_f(ss)/Φ_f(sol) values of 7-diethylamino derivatives **2** (0.31), **4** (0.46), and **5** (0.35) were extremely higher than those of 7-amino derivatives **1** (0.01) and **3** (0.01). 4-Methyltetramethyljulolydyl derivative **7** showed larger Φ_f(ss)/Φ_f(sol) (0.36) value than 4-methyljulolydyl derivative **6** (0.04). 4-(Perfluoroalkyl)tetramethyljulolydyl derivatives **8** (0.11) and **9** (0.13) showed medium Φ_f(ss)/Φ_f(sol) values. Thus, the solid-state fluorescence intensity drastically depends on the substituents at the 4- and 7-positions.

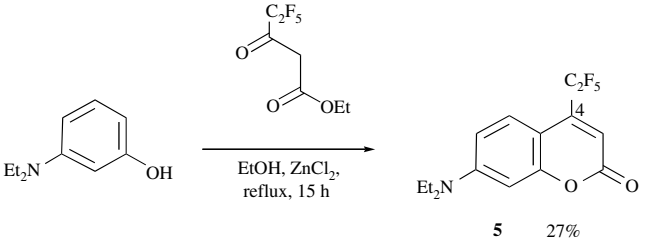

5 27%

Scheme 2. Synthesis of **5**.

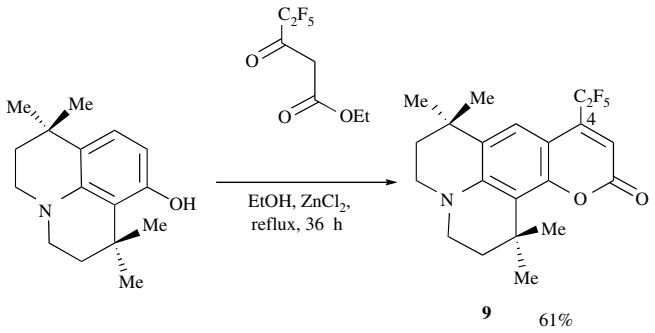

9 61%

Scheme 3. Synthesis of **9**.

2.4. X-ray crystallographic analysis of coumarin dyes

To examine the difference of solid-state fluorescence intensity among the coumarin dyes, the X-ray crystallography was performed. Coumarin dye **3** was recrystallized from ethanol. Coumarin dyes **2**, **4**–**9** were recrystallized from hexane. In the case of **1**, the reported cif file was used [26]. The results are shown in Figs. 3–10.

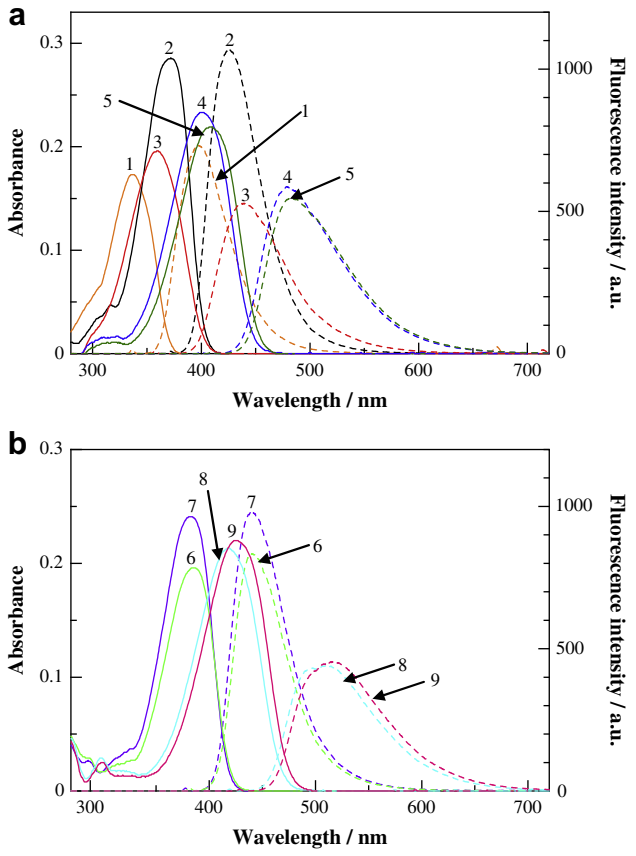

Fig. 1. UV–vis absorption and fluorescence spectra of coumarin dyes **1**–**9** in dichloromethane. Measured on 1×10^{-5} mol dm^{-3} of substrate at 25 °C. Solid and dotted lines represent UV–vis absorption and fluorescence spectra, respectively.

Table 1
UV–vis absorption and fluorescence spectra of **1**–**9**.

Compd	In dichloromethane[a]					Solid state			Φ_f(ss)/Φ_f(sol)
	λ_{max} (ε) (nm)	λ_{ex} (nm)	F_{max} (nm)	Φ_f(sol)[b]	Stokes shift (nm)	λ_{ex}[c] (nm)	F_{max} (nm)	Φ_f(ss)[d]	
1	336 (17,300)	335	397	0.82	61	360	450	0.01	0.01
2	372 (24,100)	370	424	0.95	52	385	432	0.29	0.31
3	360 (19,600)	356	439	0.83	79	385	476	0.01	0.01
4	401 (23,300)	398	478	0.87	77	405	522	0.40	0.46
5	409 (21,900)	408	480	0.86	71	410	512	0.30	0.35
6	385 (19,600)	380	440	0.93	56	390	471	0.04	0.04
7	382 (24,100)	376	441	0.94	59	390	494	0.34	0.36
8	417 (21,300)	418	510	0.80	93	430	541	0.09	0.11
9	426 (22,000)	427	517	0.77	91	435	551	0.10	0.13

[a] Measured at the concentration of 1.0×10^{-5} mol dm^{-3} at 25 °C.
[b] Determined using quinine sulfate in 0.1 mol dm^{-3} sulfuric acid as a reference ($F_f = 0.55$, $\lambda_{max} = 366$ nm) at 25 °C.
[c] Obtained by measuring diffuse reflectance spectra given in Kubelka-Munk units.
[d] Determined by a Hamamatsu Photonics Absolute PL Quantum Yield Measurement System C9920-02.

Fig. 3 shows the X-ray crystallography of **1**. Molecules are arranged as slipped parallel. Fig. 3b depicts that molecule A is surrounded by B, C, D, and E. Molecules A and D form a pair of head-to-tail dimer with two hydrogen bonds (N(1)–O(2)) and two CH/O interactions (C(7)–O(1)). Molecules A, B, and C are located on the same plane and aligned toward same direction. A hydrogen bond (N(1)–O(2)) is also observed between A and B. The same interaction is observed between A and C. Fig. 3c shows that molecule D is not located on the same plane with A. The interplanar distance between A and E and A and G is 3.457 and 3.461 Å, respectively. Fig. 3d clearly indicates that molecules A, E, and G are completely overlapped and strong π–π interactions are observed among them. Thus, coumarin dye **1** has network hydrogen bonds, CH/O, and strong network π–π interactions.

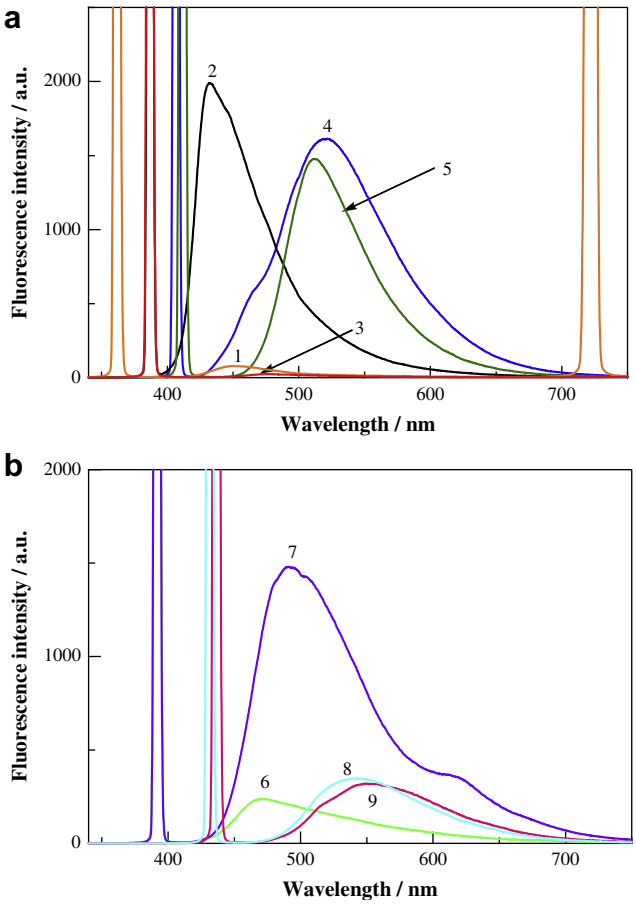

Fig. 2. Solid-state fluorescence of coumarin dyes **1**–**9**. λ_{ex} was obtained by measuring diffuse reflectance spectra given by Kubelk–Munk units.

The X-ray crystallographic analysis of **2** is shown in Fig. 4. Coumarin dye **2** is arranged as a "herring-bone" fashion. Fig. 4b shows that molecule A is surrounded by B, C, D, E, and F. Only one interaction, in which atomic distance is shorter than 3.6 Å, is observed between A and B with CH/O interaction (C(10)–O(2)). Weak CH/O (C(13)–O(2)) and CH/π (C(14)–C(8)) interactions are observed between A and C. CH/π interactions (C(7)–C(10) and C(6)–C(10)) are observed between A and F. The tilt angle between A and F is 61°, indicating weak edge-to-face interactions between them. Though molecules A, B, and G are arranged in parallel, no π–π overlapping is observed among them as shown in Fig. 4c. Thus, coumarin dye **2** has isolated monomer-type stacking having little interactions with adjacent molecules.

In compound **3**, molecules are arranged as slipped parallel. Molecule A is surrounded by B, C, D, E, F, and G as shown in Fig. 5b. Molecules A and D form a pair of head-to-tail dimer and are located almost on the same plane. Two hydrogen bonds (N(1)–O(2)) and two CH/O interactions (C(8)–O(1)) are observed between A and D. Molecules A, B, and C are located on the same plane and are aligned toward same direction. Hydrogen bonds (N(1)–O(2)) are observed among A, B, and C. Interestingly, F/F interaction (F(2)–F(3)) is also observed between A and G. Fig. 5c shows that molecules A, E, and F are arranged in parallel, there being the interplanar distance 3.322 and 3.310 Å, respectively. There is a little π–π overlapping among them as shown in Fig. 5d. Thus, coumarin dye **3** has network hydrogen bonds, CH/O, F/F, and a little π–π interactions.

Coumarin dye **4** forms a pair of head-to-tail dimer in the crystalline. These dimers are arranged as a "herring-bone" fashion. Fig. 6b and c shows that a pair of dimer A and B is formed by strong π–π interactions, there being the interplanar distance 3.529 Å. Additional CH/O interaction (C(14)–O(2)) is observed between A and B. Interestingly, this pair of dimer has no intense interactions with adjacent dimer pairs except for weak CH/π (C(13)–C(4) and C(11)–C(7)) ones. Thus, coumarin dye **4** has isolated dimer-type stacking.

Coumarin dye **5** has similar molecular packing to **4**. A pair of head-to-tail dimers is arranged as a "herring-bone" fashion. Strong π–π interactions are observed between A and B, there being the interplanar distance 3.458 Å with intense overlapping as shown in Fig. 7b and c. The pair of dimer has no strong interactions with adjacent dimer pairs. Thus, coumarin dye **5** also has isolated dimer-type stacking.

Compound **6** is arranged as a "bricks-in-a-wall" fashion as shown in Fig. 8b. The julolydyl moiety is not as bulky as supposed.

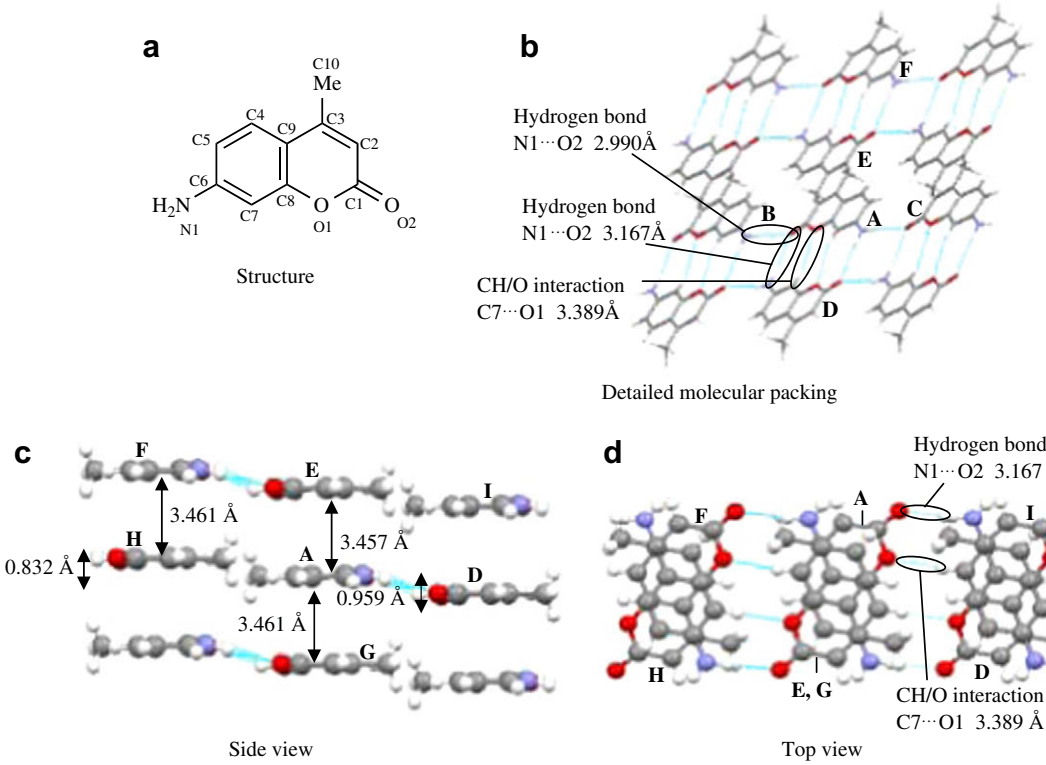

Fig. 3. X-ray crystallography of **1**.

Molecules A, B, and C are located almost in the same plane as shown in Fig. 8c. Fig. 8d shows that molecule A has CH/O interaction (C(14)–O(2)) with C to form a dimer. Molecules A, D, and E are arranged in parallel, there being the interplanar distance 3.609 Å. Fig. 8d shows that there are strong network π–π stacking among A, D, and E.

Compound **7** is arranged as a "herring-bone" fashion. Molecules A and B are packed in parallel with CH/O (C(17)–O(2)) and CH/π

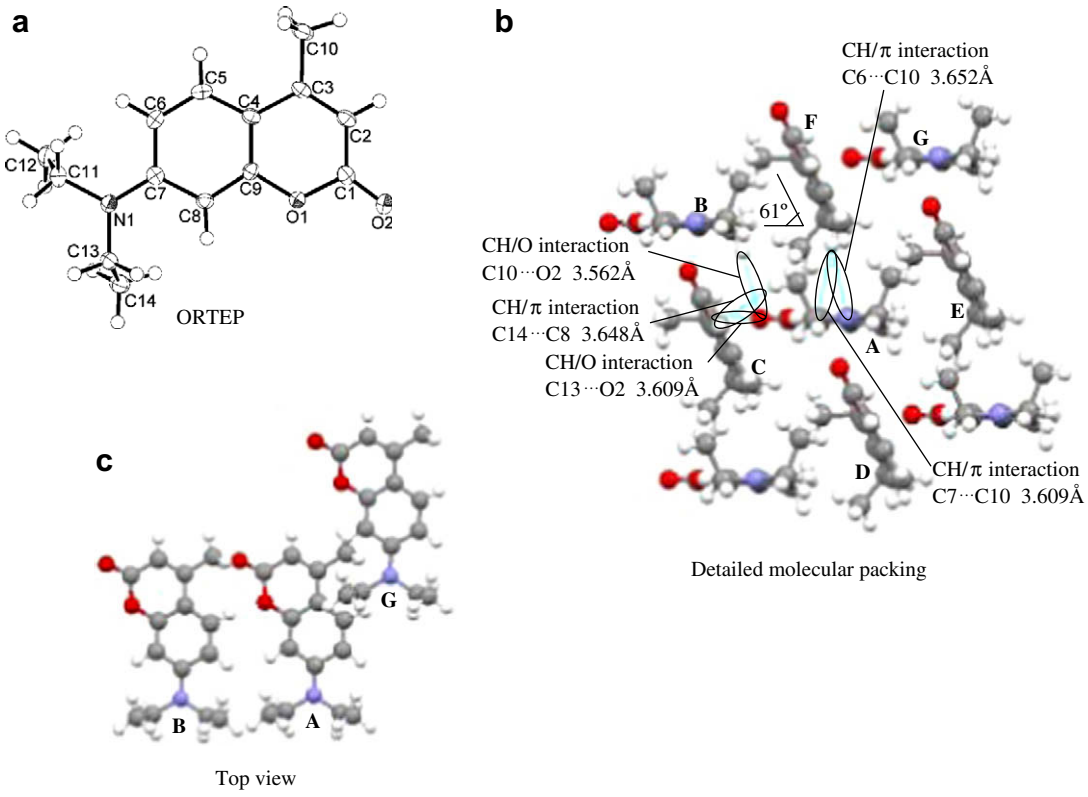

Fig. 4. X-ray crystallography of **2**.

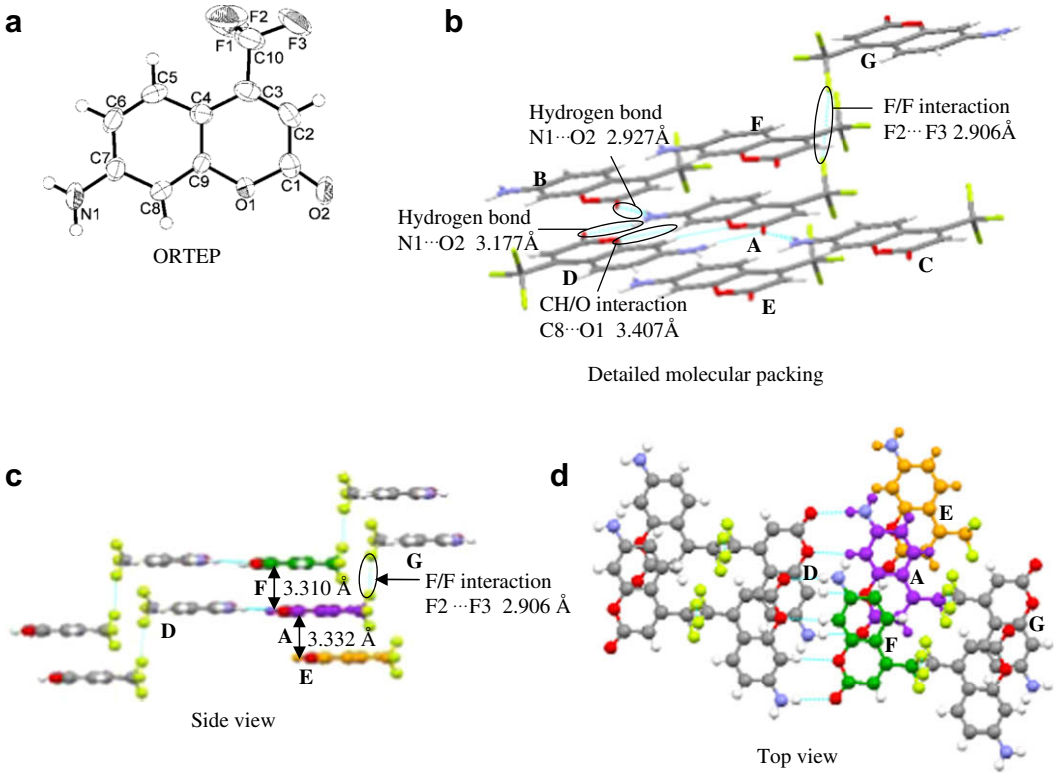

Fig. 5. X-ray crystallography of **3**.

(C(20)–C(9) and C(20)–C(3)) interactions as shown in Fig. 9b and c. Fig. 9d shows that molecule A may considerably overlap with B. However, the interplanar distance (4.509 Å) between A and B is too long to show π–π interactions. Molecule A also has CH/π interaction (C(12)–C(9)) with C. The same interaction is observed between A and D. The tilt angle between A and D is 34°. Thus, molecule A has no π–π interactions with B and has little interactions with adjacent molecules C and D. Thus, compound **7** has monomer-type packing.

The X-ray crystallography of **8** is shown in Fig. 10. This compound has two planes, in which molecules are packed in parallel. They are alternatively arranged in perpendicular in the crystalline. There are two molecules A and E which are packed

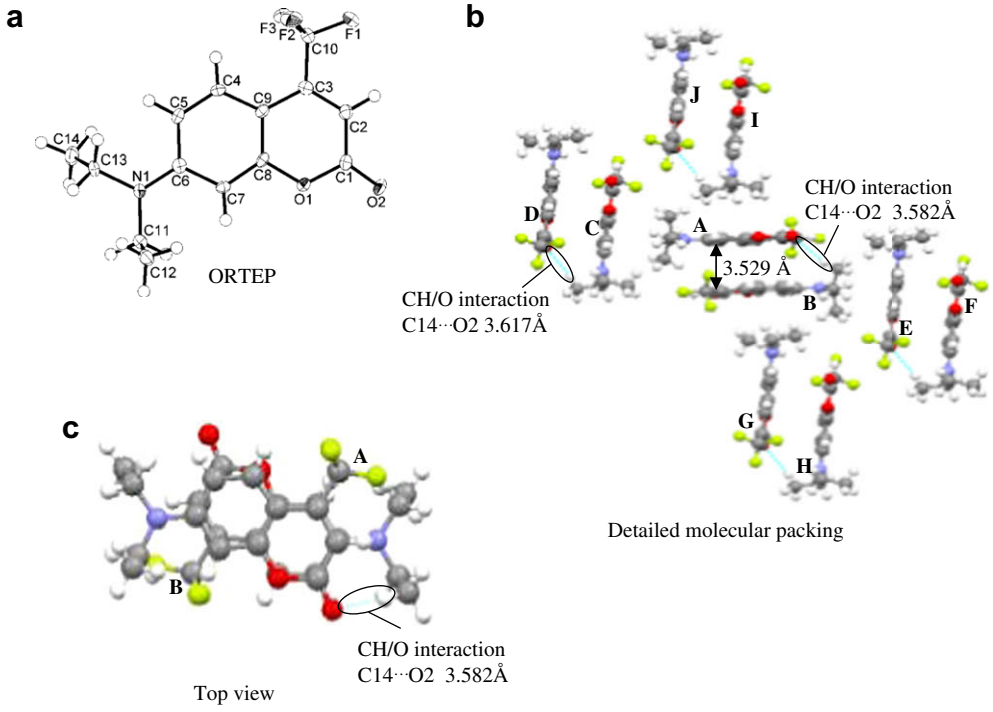

Fig. 6. X-ray crystallography of **4**.

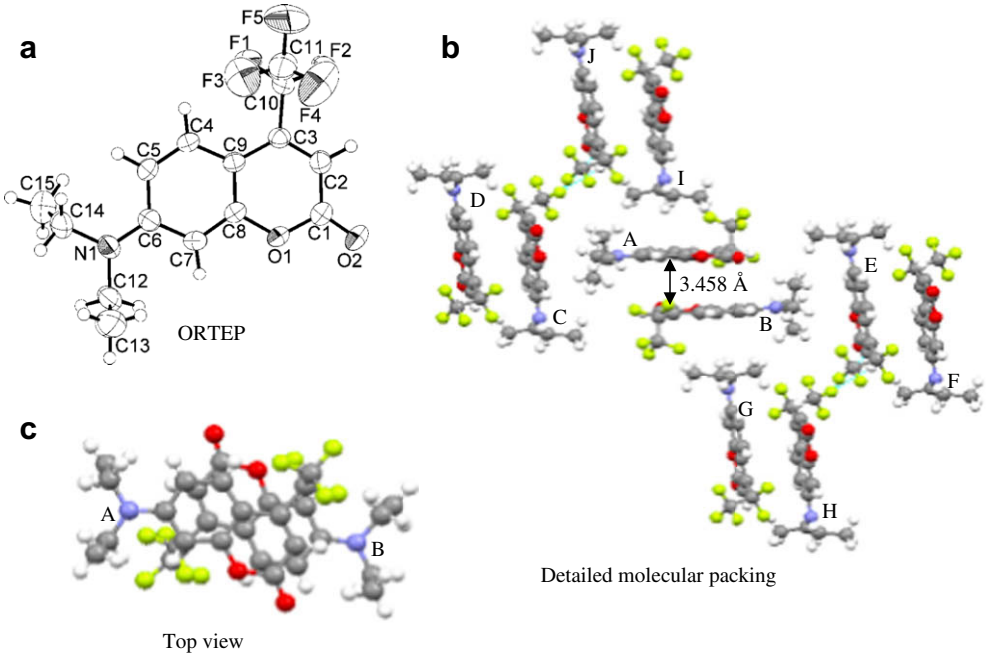

Fig. 7. X-ray crystallography of **5**.

under different circumstances in the crystalline. Molecule A is surrounded by B, C, D, E, and F as shown in Fig. 10b. Molecule A has CH/O (C(2)–O(2)) interaction with D. It also has CH/π (C(17)–C(6)) and CH/F (C(13)–F(3)) interactions with E. The tilt angle between A and E is 36°. Molecule A is packed in parallel for B with interplanar distance 4.518 Å, which is too long to show π–π interactions between them. Fig. 10c and d shows that CH/F and CH/O interactions are observed between H and I and I and J, respectively. These molecules arranged almost in parallel have network CH/O and CH/F interactions. Thus, compound **8** has isolated monomer-type packing with some intermolecular interactions.

As the packing of **4** and **5** consists of isolated dimer-type stacking, the fluorescence may come from the excimer. The time-resolved fluorescence spectrum of **4** is shown in Fig. 11. The decay curve suggests that there are two components in the emission. Though no clear bathochromic emission was observed, two components having the lifetime 6.5 and 18.5 ns were observed in 57 and 43%, respectively. That of **5** also indicated two components

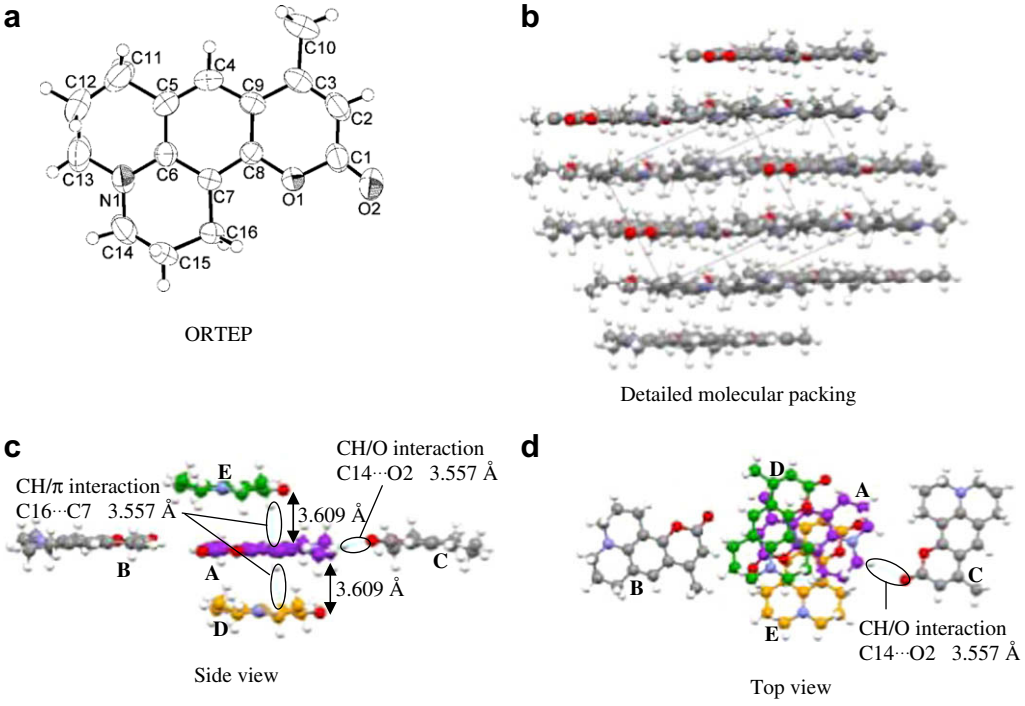

Fig. 8. X-ray crystallography of **6**.

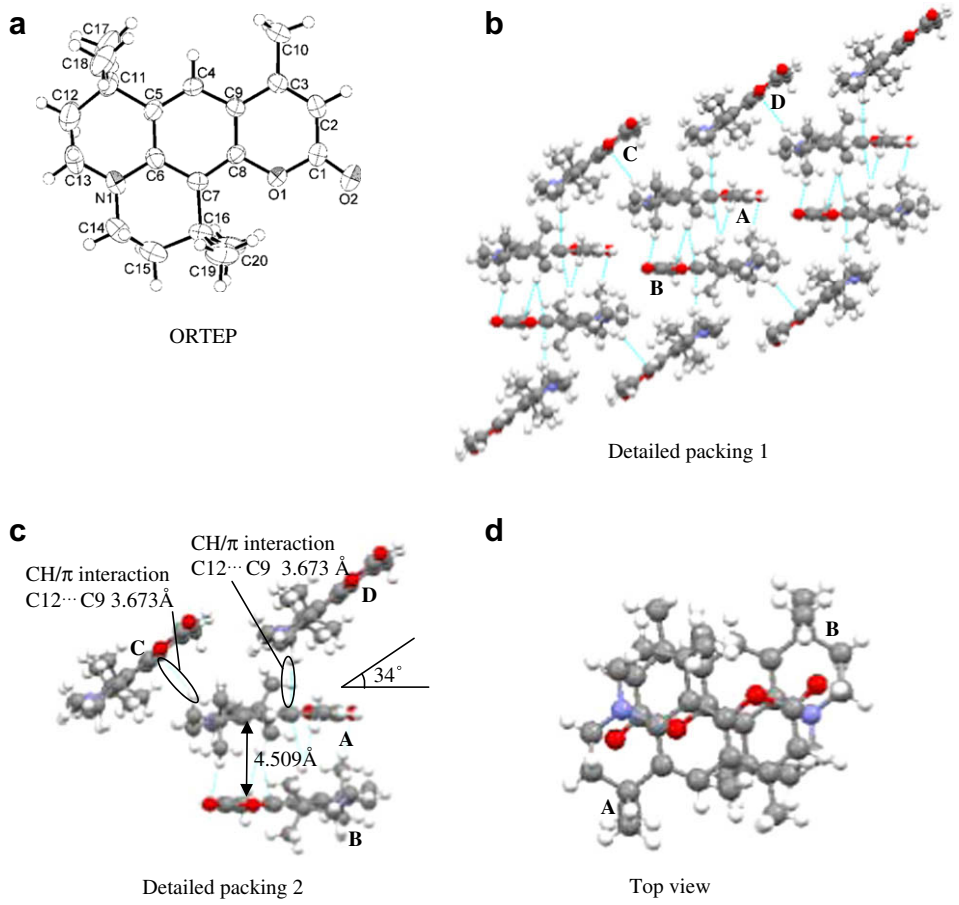

Fig. 9. X-ray crystallography of **7**.

(6.2 ns (43%), 13.1 ns (57%)). These results suggest that both the emission from monomer and excimer are contained in the fluorescence of **4** and **5**.

The solid-state fluorescence spectra in potassium bromide in the range of 0.001 mol% of **4** to neat form showed slight bathochromic shift in the fluorescence spectra as shown in Fig. 12. This result suggests that emission band from excimer of **4** is very close to that of monomer.

Fig. 13 shows solid-state fluorescence of coumarin dyes. It is clear that the solid-state fluorescence intensity is drastically affected by changing the substituents at the 4- and 7-positions.

3. Conclusions

The relationship between solid-state fluorescence and molecular packing of typical coumarin dyes was systematically examined. They showed F_{max} in the range of 432–551 nm. Interestingly, the Φ_f(ss) significantly changed by the kinds of substituents at the 4- and 7-positions. The relationship between the molecular packing and Φ_f(ss) is classified into five types:

1) network hydrogen bond type 7-aminocoumarins such as **1** and **3** showing low Φ_f(ss).
2) isolated monomer-type coumarins **2** and **7** showing high Φ_f(ss).
3) isolated dimer-type 7-diethylamino-4-(perfluoroalkyl)coumarins **4** and **5** showing high Φ_f(ss) from both monomer and excimer.
4) π–π stacking type 4-methyl-substituted julolydylcoumarin **6** showing low Φ_f(ss).
5) isolated monomer-type 4-(perfluoroalkyl)tetramethyljulolydyl coumarins **8** and **9** with some intermolecular interactions showing medium Φ_f(ss).

4. Experimental

4.1. General

Melting points were measured with a Yanagimoto MP-52 micro-melting-point apparatus and SII Technology Co., EXSTAR-6000 instrument. NMR spectra were obtained by a JEOL ECX 400P spectrometer. MS spectra were measured with a JEOL MStation 700 spectrometer. Elemental analysis was performed with a Yanaco MT-6 CHN corder. UV–vis absorption and fluorescence spectra were taken on Hitachi U-3500 and F-4500 spectrophotometers, respectively. Fluorescence quantum yield in solid state was measured by a Hamamatsu Photonics Absolute PL Quantum Yield Measurement System C9920-02. 3-(Diethylamino)phenol, ethyl (pentafluoropropanoyl)acetate, 7-amino-4-methylcoumarin (**1**), and 7-amino-4-(trifluoromethyl)coumarin (**3**) were purchased from Tokyo Kasei Co., Ltd. 2,3,6,7-Tetrahydro-1*H*,5*H*-benzo[*ij*]quinolizin-8-ol [27], 2,3,6,7-tetrahydro-1,1,7,7-tetramethyl-1*H*,5*H*-benzo[*ij*]quinolizin-8-ol [28], 7-diethylamino-4-methylcoumarin (**2**) [25], and 7-diethylamino-4-(trifluoromethyl)coumarin (**4**) [29] were synthesized as described in literature. All the coumarin dyes were recrystallized and sublimed for purification.

4.2. Synthesis of 7-diethylamino-4-(pentafluoroethyl)coumarin (*5*)

To ethanol (15 ml) were added 3-(diethylamino)phenol (12 mmol), ethyl (pentafluoropropanoyl)acetate (14 mmol), and anhydrous zinc chloride (15 mmol). The mixture was refluxed for 15 h. After the reaction was completed, the mixture was poured

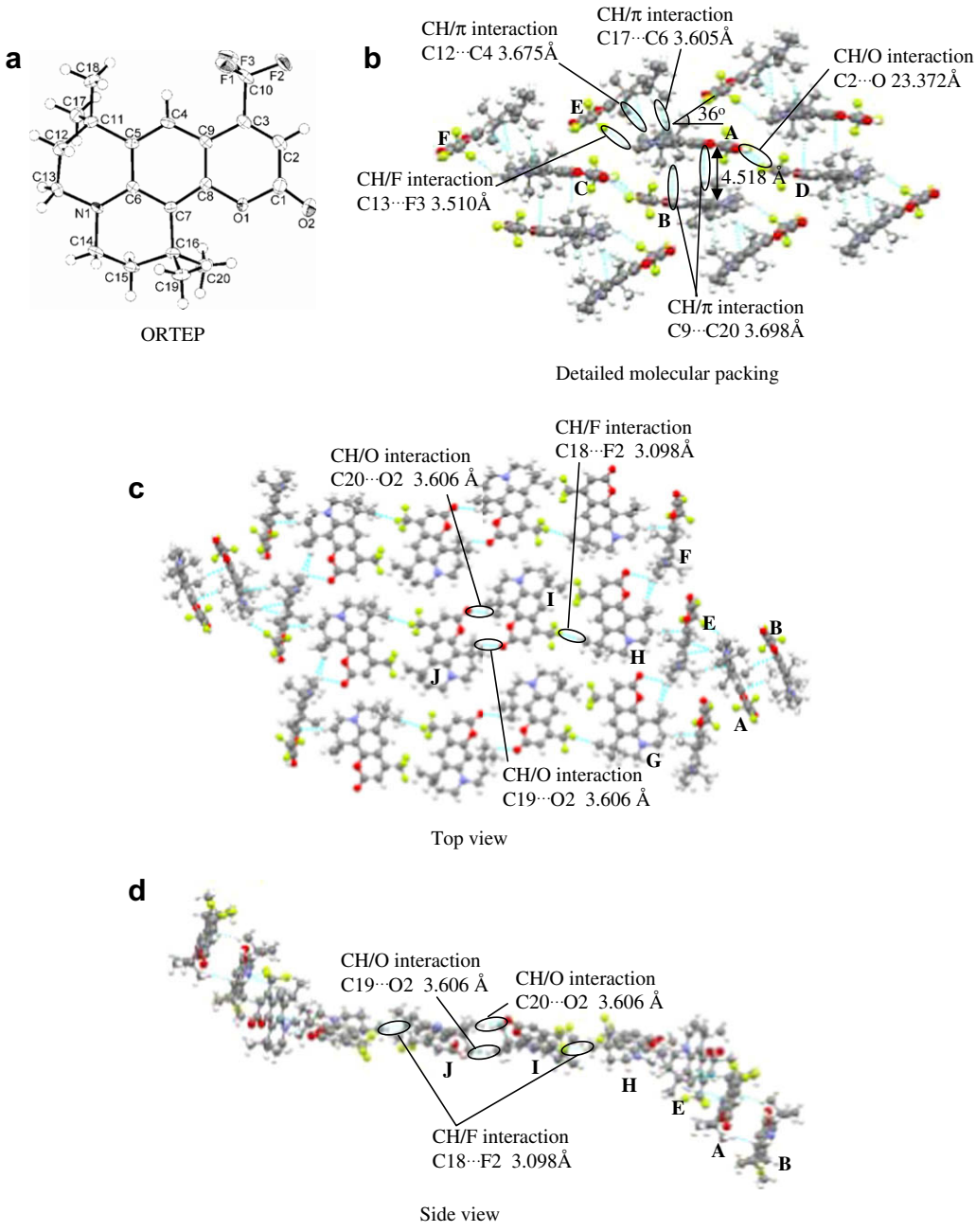

Fig. 10. X-ray crystallography of **8**.

into aqueous hydrochloric acid (0.1 mol dm^{-3}, 50 ml). The product was extracted with dichloromethane (30 ml × 3). The extract was washed with water (30 ml × 3) and concentrated *in vacuo*. The product was purified by column chromatography (silica gel, dichloromethane), recrystallized from hexane, and sublimed. The physical and spectral data are shown below. Yield 27%; mp 82–83 °C; ^{1}H NMR ($CDCl_3$) $\delta = 1.23$ (t, $J = 7.2$ Hz, 6H), 3.43 (q, $J = 7.2$ Hz, 4H), 6.35 (s, 1H), 6.53 (d, $J = 2.7$ Hz, 1H), 6.61 (dd, $J = 9.3$ and 2.7 Hz, 1H), 7.53 (d, $J = 9.3$ Hz, 1H); EIMS (70 eV) *m/z* (rel intensity) 335 (M^+, 9), 320 (36), 292 (100), 264 (19). Anal: Found: C, 53.82; H, 4.38; N, 4.24%. Calcd for $C_{15}H_{14}NO_2$: C, 53.74; H, 4.21; N, 4.18%.

4.3. Synthesis of coumarin dyes **6**–**9**

To ethanol (10 ml) were added 2,3,6,7-tetrahydro-1*H*,5*H*-benzo[*ij*]quinolizin-8-ols **1** and **2** (4.08 mmol), ethyl acylacetates **3**–**5** (4.5 mmol), and anhydrous zinc chloride (4.9 mmol). The mixture was refluxed (**6**: 12 h, **7**: 15 h, **8**: 24 h, **9**: 36 h). After the reaction was completed, the mixture was poured into aqueous hydrochloric acid (0.1 mol dm^{-3}, 50 ml). The product was extracted with dichloromethane (50 ml × 3). The extract was washed with water (70 ml × 3) and concentrated *in vacuo*. The product was purified by silica gel column chromatography (**6**: dichloromethane, **7**: ether:hexane = 5:3, **8**: dichloromethane, **9**: dichloromethane), recrystallized from hexane, and sublimed. The physical and spectral data are shown below.

4.3.1. 2,3,6,7-Tetrahydro-9-methyl-1H,5H-quinolizino[9,-1-gh]coumarin (**6**)

Yield 85%; mp 154.1 °C (94–96 °C [24]); ^{1}H NMR ($CDCl_3$) $\delta = 1.96$–2.00 (m, 4H), 2.31 (s, 3H), 2.78 (t, $J = 6.4$ Hz, 2H), 2.89 (t, $J = 6.4$ Hz, 2H), 3.24 (t, $J = 5.6$ Hz, 2H), 3.26 (t, $J = 5.6$ Hz, 2H), 5.91 (s, 1H), 6.98 (s, 1H); EIMS (70 eV) *m/z* (rel intensity) 255 (M^+: 100),

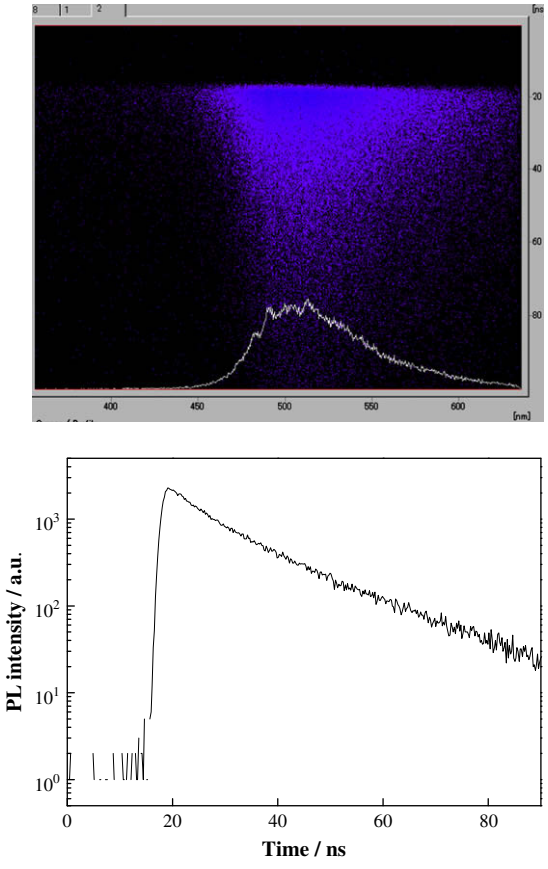

Fig. 11. Time-resolved fluorescence spectrum of **4** in solid state.

226 (27). Anal: Found: C, 74.75; H, 6.75; N, 5.38%. Calcd for $C_{16}H_{17}NO_2$: C, 75.27; H, 6.71; N, 5.49%. There is a big difference between observed and reported melting point. The TG-DTA of **6** showed its melting point at 154.1 °C.

*4.3.2. 2,3,6,7-Tetrahydro-1,1,7,7,9-pentamethyl-1*H,5H,*11*H-*[1]benzopyrano-[6,7,8-ij]quinolizin-11-one (**7**)*

Yield 76%; mp 173.7 °C (149–151 °C [30]); ^{1}H NMR ($CDCl_3$) $\delta = 1.31$ (s, 6H), 1.55 (s, 6H), 1.75–1.77 (m, 2H), 1.80–1.82 (m, 2H), 2.33 (s, 3H), 3.18–3.20 (m, 2H), 3.26–3.29 (m, 2H), 5.92 (s, 1H), 7.23 (s, 1H); EIMS (70 eV) *m*/*z* (rel intensity) 311 (M^+, 73), 296 (100). Anal: Found: C, 77.04;H, 7.87; N, 4.47%. Calcd for $C_{20}H_{25}NO_2$: C, 77.14; H, 8.09; N, 4.50%. There is a big difference between observed and reported melting point. The TG-DTA of **7** showed its melting point at 173.7 °C.

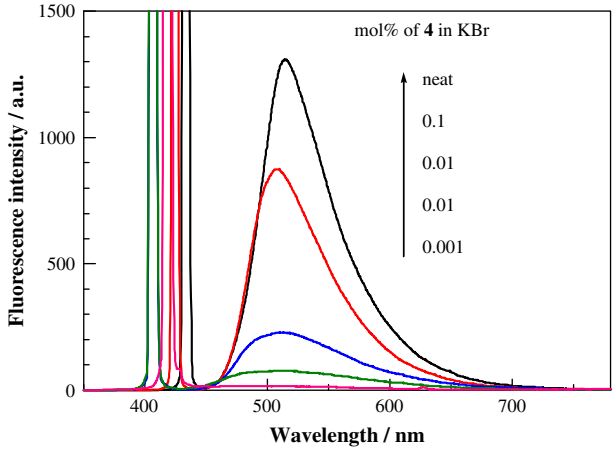

Fig. 12. Fluorescence spectra of **4** from 0.001 mol% in potassium bromide to neat form.

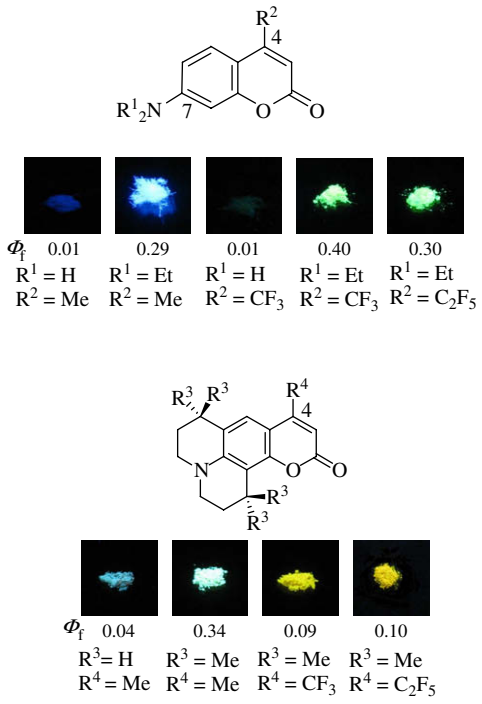

Fig. 13. Solid-state fluorescence of coumarin dyes irradiated with black light (254 nm).

*4.3.3. 2,3,6,7-Tetrahydro-1,1,7,7-tetramethyl-9-trifluoromethyl-1*H,5H,*11*H-*[1]-benzopyrano[6,7,8-ij]quinolizin-11-one (**8**)*

Yield 50%; mp 105–106 °C (106–107 °C [30]); ^{1}H NMR ($CDCl_3$) $\delta = 1.29$ (s, 6H), 1.53 (s, 6H), 1.73–1.76 (m, 2H), 1.79–1.82 (m, 2H), 3.22–3.25 (m, 2H), 3.30–3.33 (m, 2H), 6.32 (s, 1H), 7.32 (d, $J = 1.8$ Hz, 1H); EIMS (70 eV) *m*/*z* (rel intensity) 365 (M^+: 41), 350 (100), 294 (86), 266 (67).

*4.3.4. 2,3,6,7-Tetrahydro-1,1,7,7-tetramethyl-9-pentafluoroethyl-1*H,5H,*11*H-*[1]-benzopyrano[6,7,8-ij]quinolizin-11-one (**9**)*

Yield 61%; mp 155–156 °C; ^{1}H NMR ($CDCl_3$) $\delta = 1.54$ (s, 6H), 1.57 (s, 6H), 1.74–1.77 (m, 2H), 1.80–1.83 (m, 2H), 3.23–3.26 (m, 2H), 3.31–3.34 (m, 2H), 6.32 (s, 1H), 7.40 (s, 1H); EIMS (70 eV) *m*/*z* (rel intensity) 415 (M^+, 55), 400 (100). Anal: Found: C, 60.37; H, 5.40; N, 3.39%. Calcd for $C_{21}H_{22}N_5O_2$: C, 60.72; H, 5.34; N, 3.37%.

4.4. X-ray crystallographic analysis

Single crystals were grown by a solvent diffusion method using hexane and dichloromethane. The diffraction data were collected by a Rigaku AFC7R Mercury CCD diffractometer using graphite monochromated Mo-K_α radiation ($\lambda = 0.71069$ Å). The structure was solved by direct methods SIR97, and refined by fill-matrix least-squares calculations. Crystal data for **2**: $C_{14}H_{17}NO_2$, $Mw = 231.29$, monoclinic, $P21$, $Z = 2$, $a = 8.947(8)$, $b = 6.975(6)$, $c = 9.821(9)$ Å, $\alpha = 90$, $\beta = 90.796(11)$, $\gamma = 90°$, $D_{calcd} = 1.253$ g cm^{-3}, $T = 123(2)$ K, $F(000) = 248$, $\mu = 0.084$ mm^{-1}, 4930 reflections were corrected, 2294 unique ($R_{int} = 0.0356$). 2294 observed ($I > 2\sigma$ (I)), 157 parameters, $R_1 = 0.0511$, $wR_2 = 0.0961$. Crystal data for **3**: $C_{10}H_6F_3NO2$, $Mw = 229.16$, triclinic, P-1, $Z = 2$, $a = 5.193(7)$, $b = 6.890(9)$, $c = 14.16(2)$ Å, $\alpha = 82.84(4)$, $\beta = 85.59(4)$, $\gamma = 72.70(3)°$, $D_{calcd} = 1.587$ g cm^{-3}, $T = 123(2)$ K, $F(000) = 232$,

$\mu = 0.149\ mm^{-1}$, 3971 reflections were corrected, 2160 unique ($R_{int} = 0.0473$). 2160 observed ($I > 2\sigma\ (I)$), 169 parameters, $R_1 = 0.1163$, $wR_2 = 0.2193$. Crystal data for **4**: $C_{56}H_{56}F_{12}N_4O_8$, $Mw = 1141.05$, triclinic, P-1, $Z = 2$, $a = 10.004(6)$, $b = 14.283(8)$, $c = 18.557(11)$ Å, $\alpha = 85.605(13)$, $\beta = 89.767(14)$, $\gamma = 80.263(13)^\circ$, $D_{calcd} = 1.454\ g\ cm^{-3}$, $T = 123(2)$ K, $F(000) = 1184$, $\mu = 0.126\ mm^{-1}$, 21,478 reflections were corrected, 11,826 unique ($R_{int} = 0.0491$). 11,826 observed ($I > 2\sigma\ (I)$), 730 parameters, $R_1 = 0.0956$, $wR_2 = 0.1359$. Crystal data for **5**: $C_{15}H_{14}F_5NO_2$, $Mw = 335.27$, monoclinic, $P2_1/c$, $Z = 8$, $a = 10.658(6)$, $b = 19.289(9)$, $c = 15.868(8)$ Å, $\alpha = 90$, $\beta = 112.021(6)$, $\gamma = 90^\circ$, $D_{calcd} = 1.473\ g\ cm^{-3}$, $T = 286(2)$ K, $F(000) = 1376$, $\mu = 0.138\ mm^{-1}$, 24,477 reflections were corrected, 6909 unique ($R_{int} = 0.0435$). 6906 observed ($I > 2\sigma\ (I)$), 499 parameters, $R_1 = 0.0942$, $wR_2 = 0.1488$. Crystal data for **6**: $C_{16}H_{17}NO_2$, $Mw = 255.31$, monoclinic, $P2_1/a$, $Z = 4$, $a = 8.260(6)$, $b = 15.670(10)$, $c = 10.130(7)$ Å, $\alpha = 90$, $\beta = 95.770(9)$, $\gamma = 90^\circ$, $D_{calcd} = 1.300\ g\ cm^{-3}$, $T = 296(2)$ K, $F(000) = 544$, $\mu = 0.086\ mm^{-1}$, 10,314 reflections were corrected, 2955 unique ($R_{int} = 0.0345$). 2955 observed ($I > 2\sigma\ (I)$), 217 parameters, $R_1 = 0.0952$, $wR_2 = 0.2180$. Crystal data for **7**: $C_{20}H_{25}NO_2$, $Mw = 311.41$, monoclinic, $P2_1/n$, $Z = 4$, $a = 11.3454(14)$, $b = 10.3138(11)$, $c = 14.7881(18)$ Å, $\alpha = 90$, $\beta = 94.177(6)$, $\gamma = 90^\circ$, $D_{calcd} = 1.199\ g\ cm^{-3}$, $T = 296(2)$ K, $F(000) = 672$, $\mu = 0.077\ mm^{-1}$, 13,380 reflections were corrected, 3907 unique ($R_{int} = 0.0274$). 3907 observed ($I > 2\sigma\ (I)$), 271 parameters, $R_1 = 0.0845$, $wR_2 = 0.2170$. Crystal data for **8**: $C_{20}H_{22}F_3NO_2$, $Mw = 365.39$, monoclinic, $P2_1/n$, $Z = 8$, $a = 9.785(2)$, $b = 38.181(6)$, $c = 10.372(2)$ Å, $\alpha = 90$, $\beta = 112.436(8)$, $\gamma = 90^\circ$, $D_{calcd} = 1.355\ g\ cm^{-3}$, $T = 123(2)$ K, $F(000) = 1536$, $\mu = 0.108\ mm^{-1}$, 21,246 reflections were corrected, 7652 unique ($R_{int} = 0.1377$). 7652 observed ($I > 2\sigma\ (I)$), 477 parameters, $R_1 = 0.1292$, $wR_2 = 0.2360$. Crystallographic data (**2** (CCDC 690559), **3** (CCDC 690557), **4** (CCDC 690558), **5** (CCDC 689391), **6** (CCDC 696813), **7** (CCDC 696815), **8** (CCDC 696814)) have been deposited at the CCDC, 12 Union Road, Cambridge CB2 1EZ, UK.

Acknowledgements

The authors are grateful to Prof. Dr. Chihaya Adachi and Mr. Ayataka Endoh of center for future chemistry, Kyushu University, for time-resolved fluorescence spectral measurements.

References

[1] Shirai K, Matsuoka M, Matsumoto S, Shiro M. Molecular stacking and solid state spectra of 2,5-bis(1-aza-1-cycloalkyl)-3,6-dicyanopyrazines and their X-ray crystal structures. Dyes Pigment 2003;56:83–7.
[2] Mizuyama N, Tominaga Y, Kohra S, Ueda K, Hirayama S, Shigemitsu Y. Synthesis and steady-state spectroscopic study of 5-aryl-2,2′-bipyridyls. New fluorescent compounds in solid state. Bull Chem Soc Jpn 2006;79:602–11.
[3] Horiguchi E, Matsumoto S, Funabiki K, Matsui M. Optical properties of novel 2,3-dicyano-5-methyl-6H-1,4-diazepine dyes in the solid state. Bull Chem Soc Jpn 2005;78:1167–73.
[4] Ooyama Y, Mamura T, Yoshida Y. A facile synthesis of solid-emissive fluorescent dyes. Dialkylbenzo[b]naphtho[2,1-d]furan-6-one-type fluorophores with strong blue and green fluorescence emission properties. Tetrahedron Lett 2007;48:5791–3.
[5] Ooyama Y, Harima Y. Dramatic effects of the substituents on the solid-state fluorescence properties of structural isomers of novel benzofuro[2,3-c] oxazolocarbazole-type fluorophores. Chem Lett 2006;35:902–3.
[6] Ooyama Y, Kagawa Y, Harima Y. Synthesis and solid-state fluorescence properties of structural isomers of novel benzofuro[2,3-c]oxazolocarbazole-type fluorescent dyes. Eur J Org Chem 2007:3613–21.
[7] Ooyama Y, Mamura T, Yoshida K. Synthesis, X-ray crystal structures and solid-state fluorescence properties of 3-dibutylamino-6-alkoxy-6-phenylnaphtho[2,3-b]benzofuran-11(6H)-one derivatives. Eur J Org Chem 2007:5010–9.
[8] Yushchenko DA, Bilokin MD, Pyvovarenko OV, Duportail G, Mély Y, Pivovarenko VG. Synthesis and fluorescence properties of 2-aryl-3-hydroxyquinolones, a new class of dyes displaying dual fluorescence. Tetrahedron Lett 2006;47:905–8.
[9] Yeh HC, Wu WC, Wen YS, Dai DC, Wang JK, Chen CT. Derivative of α,β-dicyanostilbene. Convenient precursor for the synthesis of diphenylmaleimide compound, E–Z-isomerization, crystal structure, and solid-state fluorescence. J Org Chem 2004;69:6455–62.
[10] Lee YT, Chiang CL, Chen CT. Solid-state highly fluorescent diphenylaminospirobifluorenylfumaronitrile red emitters for non-doped organic light-emitting diodes. Chem Commun 2008:217–9.
[11] Radke KR, Ogawa K, Rasmussen SC. Highly fluorescent oligothiophenes through the incorporation of central dithieno[3,2-b:2′,3′-d]pyrrole units. Org Lett 2005;7:5253–6.
[12] Seo J, Kim S, Lee YS, Kwon OH, Park KH, Choi SY, et al. Enhanced solid-state fluorescence in the oxadiazole-based excited-state intramolecular proton-transfer (ESIPT) material. Synthesis, optical property, and crystal structure. J Photochem Photobiol A Chem 2007;191:51–8.
[13] Zhao CH, Wakamiya A, Inukai Y, Yamaguchi S. Highly emissive organic solids containing 2,5-diboryl-1,4-phenylene unit. J Am Chem Soc 2006; 128:15934–5.
[14] Hirano K, Minakata S, Komatsu M. Unusual fluorescent properties of novel fluorophores, 6-aryl-3,4-diphenyl-α-pyrone derivatives. Bull Chem Soc Jpn 2001;74:1567–75.
[15] Langhals H, Ismael R, Yürük O. Persistent fluorescence of perylene dyes by steric inhibition of aggregation. Tetrahedron 2000;56:5435–41.
[16] Ashis KS, Manoj K, Dilip KM, Haridas P. Photophysical investigations of the solvent polarity effect on the properties of coumarin-6 dye. Chem Phys Lett 2005;407:114–8.
[17] Katritzky AR, Narindoshvili T, Angrish P. N-(coumarin-3-ylcarbonyl)-α-amino acids: fluorescent markers for amino acids and dipeptides. Synthesis 2008:2013–22.
[18] Féau C, Klein E, Kerth P, Lebeau L. Synthesis of a coumarin-based europium complex for bioanalyte labeling. Bioorg Med Chem Lett 2007;17:1499–503.
[19] Zhang D, Zhang S, Ma D, Gulimina, Li X. Low threshold amplified spontaneous emission based on coumarin 151 encapsulated in mesoporous SBA-15. Appl Phys Lett 2006;89:231112.
[20] Jones II G, Rahman MA. Fluorescence properties of coumarin laser dyes in aqueous polymer media. Chromophore isolation in poly(methacrylic acid) hypercoils. J Phys Chem 1994;98:13028–37.
[21] Lee MT, Yen CK, Yang WP, Chen HH, Liao CH, Tsai CH, et al. Efficient green coumarin dopants for organic light-emitting devices. Org Lett 2004; 6:1241–4.
[22] Swanson SA, Wallraff GM, Chen JP, Zhang W, Bozano LD, Carter KR, et al. Stable and efficient fluorescent red and green dyes for external and internal conversion of blue OLED emission. Chem Mater 2003;15:2305–12.
[23] Chen CT, Chiang CL, Lin YC, Chan LH, Huang CH, Tsai ZW, et al. Ortho-substituent effect on fluorescence and electroluminescence of arylamino-substituted coumarin and stilbene. Org Lett 2003;5:1261–4.
[24] Frère S, Thièry V, Besson T. Microwave acceleration of the Pechmann reaction on graphite/montmorillonite K10. Application to the preparation of 4-substituted 7-aminocoumarins. Tetrahedron Lett 2001;42:2791–4.
[25] Matsui M, Shibata K, Muramatsu H, Sawada H, Nakayama M. Synthesis, fluorescence, and photostabilities of 3-(perfluoroalkyl)coumarins. Chem Ber 1992;125:467–71.
[26] Jasinski JP, Woudenberg RC. 7-Amino-4-methylcoumarin. Acta Crystallogr Sect C 1994;50:1954–6.
[27] Gompel JV, Schuster GB. Chemiluminescence of organic peroxides. Intramolecular electron-exchange luminescence from a secondary perester. J Org Chem 1987;52:1465–8.
[28] Lee CC, Hu AT. Synthesis and optical recording properties of some novel styryl dyes for DVD-R. Dyes Pigment 2003;59:63–9.
[29] Schimitschek EJ, Trias JA, Taylor M, Celto JE. New improved laser dyes for the blue–green spectral region. IEEE J Quantum Electron 1973;9:781–2.
[30] Fox JL, Chen CH. Benzopyrano(6,7,8-ij)quinolizine-11-one derivatives as laser dyes and intermediates for their preparation. US Patent 4,736,032 1988. (Chem Abstr 1988;109:75208b.).